Combinatorial control of biofilm development by quorum-sensing and nutrient-sensing regulators in *Pseudomonas aeruginosa*

Gong Chen[1], Emilia D. Lim[1], Bradford T. Winkelman[2], Jared T. Winkelman[1], Sampriti Mukherjee[1]*

[1]The University of Chicago, Department of Molecular Genetics & Cell Biology, Chicago, IL 60615, USA. [2]Trestle Biosciences, Milwaukee, WI 53211, USA.

*Correspondence to: sampriti@uchicago.edu

ABSTRACT

Pseudomonas aeruginosa is a leading cause of hospital-acquired infections and formation of sessile antibiotic-resistant communities called biofilms is required for virulence in this pathogen. Biofilm formation is modulated by various environmental stimuli including nutrient availability, and population density and composition monitored via the cell-cell communication process of quorum sensing. Previous work has shown that the RhlR quorum-sensing receptor as well as CbrA/CbrB two-component system required for nutritional adaptation repress biofilm formation. How the information encoded in multiple sensory inputs is extracted and integrated to control biofilms is largely mysterious. Here, we use biofilm analyses, RNA-seq studies, and reporter assays to explore the combined effect of information flow through the RhlR quorum-sensing and CbrA nutrient-sensing pathways on biofilm development. We find that when both RhlR and CbrA are inactive, the resulting biofilm is unstable and readily evolves into a variant that mimics the absence of RhlR. Using genetic suppressor analysis and whole genome sequencing, we have identified the carbon catabolite repression protein Crc as the molecular convergence point for quorum and nutrient sensing. Crc promotes the expression of Pel exopolysaccharide, Functional amyloid protein and Cup fimbriae components of the biofilm matrix but does so only in the absence of both RhlR and CbrA. These results uncover a regulatory link between nutritional adaption and quorum sensing with potential implications for anti-biofilm targeting strategies.

INTRODUCTION

Bacteria predominantly exist in structured communities called biofilms. Biofilms are defined as aggregates of cells that are embedded in a matrix made of extracellular polymeric substances (EPS) including exopolysaccharides, proteins, lipids and nucleic acids (Hall-Stoodley et al. 2004; Flemming et al. 2016; Karygianni et al. 2020). The EPS is crucial for the emergent properties of biofilms such as superior resilience to environmental stresses such as antimicrobials and host immune responses. Biofilm formation is a dynamic process that is governed by various intracellular and exogenous stimuli. Often, two-component signaling (TCS) systems integrate and relay the information contained in sensory cues into the control of biofilm formation (Liu et al., 2018; Prüß, 2017). TCSs are typically composed of sensor histidine kinases (HK) and partner response regulators (RR) that, via phosphorylation cascades, couple stimulus sensing to appropriate changes in behavior (Capra and Laub, 2012; Liu et al., 2019).

The opportunistic pathogen *Pseudomonas aeruginosa* forms biofilms in diverse free-living environments, such as soil and water and in host-associated environments, such as burn wounds, lungs of cystic fibrosis (CF) patients and plant tissues (Pendleton et al. 2013; Markou and Apidianakis, 2014; Manfredi et al. 2000; Kim et al. 2015). Accordingly, *P. aeruginosa* encodes a large suite of >60 TCS systems that likely allow it to respond to diverse external cues and adapt to a wide range of infection sites and environmental conditions (Wang et al. 2021). Despite decades of research, the identities of the stimuli detected by their corresponding sensor kinases and the actual processes controlled by most of these TCSs during biofilm development remain poorly understood.

One such TCS is the CbrA/CbrB TCS that is involved in nutritional adaptation and was first described in *P. aeruginosa* as a regulatory system involved in the hierarchical utilization of various carbon sources (Monteagudo-Cascales et al. 2022; Sonnleitner et al. 2009; Yeung et al. 2011; Sonnleitner et al. 2018). CbrA represents a non-canonical sensor HK as it can function as a histidine transporter via its large N-terminal transmembrane region called the SLC5 (SoLute

Carrier 5) domain as well as a HK via its C-terminal catalytic core consisting of a DHp (Dimerization and Histidine Phosphotransfer) domain and a catalytic ATP-Binding domain (Monteagudo-Cascales et al. 2022). CbrA has two putative sensor domains – SLC5 and PAS, yet the sensory stimulus activating its kinase is unknown. CbrA kinase phosphorylates its cognate RR CbrB (Fig. 1A). CbrB is an NtrC class transcription factor that possesses a REC receiver domain, a AAA+ ATPase domain and a HTH (Helix-Turn-Helix) DNA-binding domain and activates transcription from σ^{54} dependent promoters. The genes *cbrA* and *cbrB* are encoded in the same transcriptional unit. In addition to the metabolic regulation of carbon and nitrogen utilization in *P. aeruginosa*, Cbr TCS plays an important role in various virulence and virulence-related processes including biofilm formation and antibiotic resistance (Yeung, et al. 2011).

Another sensory cue commonly detected by bacteria is their population density via the chemical communication process called quorum sensing (Rutherford and Bassler, 2016). Quorum sensing relies on production of extracellular signaling molecules called autoinducers and their subsequent detection by cognate receptors (Miller and Bassler, 2001; Mukherjee and Bassler, 2019), and thereby allows groups of bacteria to coordinate their gene expression patterns in response to changes in population density and exhibit collective behaviors. Quorum sensing is crucial for biofilm development and virulence in *P. aeruginosa* (Davies et al., 1998; Rumbaugh et al., 2000; Mukherjee et al., 2017). The *P. aeruginosa* quorum-sensing circuit consists of two canonical LuxI/R pairs: LasI/R and RhlI/R (Seed et al. 1995; Pearson et al. 1995; Brint and Ohman,1995). LasI produces and LasR responds to the autoinducer 3OC12-homoserine lactone (3OC12-HSL) while RhlR binds to the autoinducer C4-HSL, the product of RhlI. *P. aeruginosa* LasI/R promotes biofilm formation (Davies *et al*, 1998; Sakuragi & Kolter, 2007). Conversely, we recently discovered that the *P. aeruginosa* quorum-sensing receptor RhlR represses biofilm formation (Mukherjee et al. 2017; Mukherjee et al. 2018).

Bacteria encounter multiple sensory cues simultaneously and must integrate information from each cue into a response. In this study, we examine how the CbrA/CbrB intersects with the

Rhl system to control biofilm formation. We find that absence of both signals – quorum sensing via RhlR and nutrient sensing via CbrA results in the formation of a hyper-rugose biofilm that appears unstable and readily gives rise to spontaneous suppressor mutations in the *crc* gene encoding for the carbon catabolite repression protein Crc. Transcriptomic profiling demonstrates that Crc promotes the expression of Pel exopolysaccharide, Functional amyloid protein and Cup fimbriae components of the biofilm matrix but does so only when both RhlR and CbrA are absent. Thus our work uncovers a new role for Crc as a master regulator of biofilm formation that allows the integration of quorum and nutritional cues.

RESULTS AND DISCUSSION

We recently discovered that the *P. aeruginosa* quorum-sensing receptor RhlR represses colony biofilm development (Mukherjee et al. 2017; Mukherjee et al. 2018). Specifically, on Congo red agar biofilm medium, wildtype (WT) *P. aeruginosa* UCBPP-PA14 (hereafter called PA14) exhibits a characteristic rugose-center/smooth-periphery colony biofilm phenotype, while the Δ*rhlR* mutant forms a hyper-rugose biofilm that expands to cover more surface area than the WT (Fig. 1B, C). Here, in addition to colony biofilms, we tested the contribution of RhlR to the formation of pellicle biofilms that assemble at the air–liquid interface of a standing broth culture. Compared to WT, the Δ*rhlR* mutant overproduces pellicle biofilms (Fig. S1A). We conclude that RhlR impedes *P. aeruginosa* biofilm formation at solid-air as well as air-liquid interfaces.

To study the role of the CbrA/CbrB TCS in *P. aeruginosa* biofilm formation, we first generated in-frame marker-less deletion of the *cbrA* gene in the PA14 strain. Similar to previous studies (Yeung et al. 2011; Wang et al. 2021), we find that the Δ*cbrA* mutant exhibits hyper-rugose colony biofilm phenotype and forms thick pellicles (Fig 1B, S1A). Although both Δ*rhlR* and Δ*cbrA* mutants appear to be hyper-rugose compared to WT PA14, the Δ*cbrA* mutant exhibits increased biofilm height, defined as the maximum vertical rise from the base of the colony, as opposed to

the increased surface area coverage of the Δ*rhlR* mutant (Fig. 1C, D). To confirm that the Δ*cbrA* mutant biofilm phenotypes are a consequence of the absence of information flow from CbrA kinase to CbrB response regulator, we generated a Δ*cbrB* mutant and a *cbrA*^{H766A} mutant where the histidine residue that undergoes autophosphorylation is changed to alanine to abolish kinase function of CbrA. Both the Δ*cbrB* and *cbrA*^{H766A} mutants have identical biofilm phenotype to the Δ*cbrA* mutant (Fig. S1B). Introduction of a plasmid expressing *cbrA* under its native promoter to the Δ*cbrA* and *cbrA*^{H766A} mutants restored biofilm formation to wildtype (WT) levels (Fig. 1B-D, S1B). These current analyses confirm that every component of our system is functional.

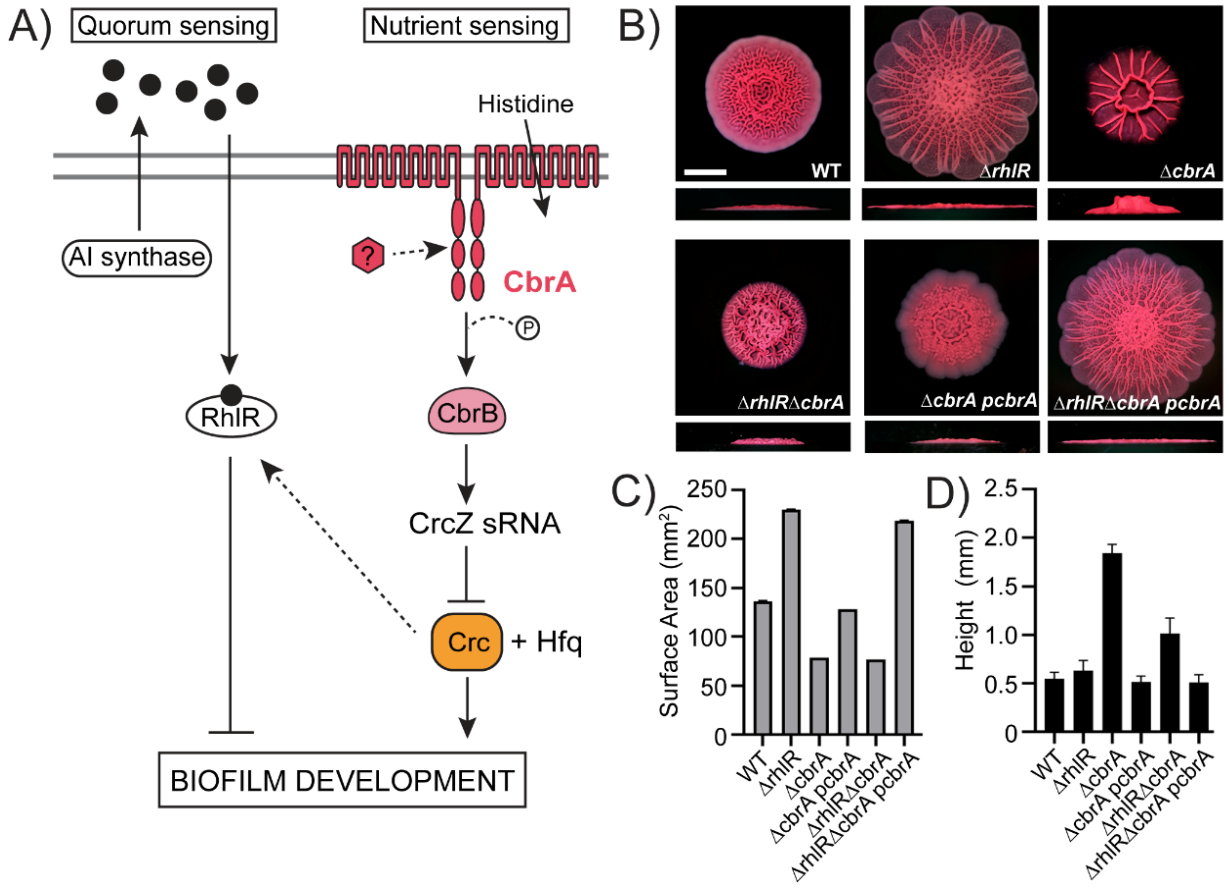

Fig. 1: *P. aeruginosa* Δ*rhlR* and Δ*cbrA* mutants have distinct hyper-rugose biofilm phenotypes. A) Schematic of the RhlR quorum sensing and CbrA nutrient sensing pathways. The two gray horizontal lines represent the cytoplasmic membrane, black circles represent autoinducer sensed by RhlR, red hexagone represents the unknown signal that activates CbrA sensor kinase. CbrA also functions as a transporter of histidine but its kinase functions appears to be independent of histidine transport (Monteagudo-Cascales et al. 2022). B) Colony biofilm phenotypes of WT PA14 and the designated mutants on Congo red agar medium after 120 h of

growth. Scale bar, 5 mm. C) Colony biofilm surface area quantitation for the indicated strains after 120 h of growth. Error bars represent SEM of three independent experiments. D) Colony biofilm height quantitation for the indicated strains after 120 h of growth. Error bars represent SEM of three independent experiments.

To explore the combined effect of Rhl and Cbr pathways on biofilm development, we deleted *rhlR* and *cbrA* together. The Δ*rhlR*Δ*cbrA* double mutant produced thick pellicles similar to Δ*rhlR* and Δ*cbrA* mutants but formed colony biofilms markedly distinct from those of the single Δ*rhlR* and Δ*cbrA* mutants: its surface area coverage mirrors the Δ*cbrA* mutant while its height is similar to the Δ*rhlR* mutant. Introduction of a plasmid expressing *cbrA* under its native promoter to the Δ*rhlR*Δ*cbrA* double mutant resulted in a hyper-rugose biofilm that is phenotypically identical to the Δ*rhlR* mutant in terms of biofilm morphology, surface area and height (Fig. 1B-D). We conclude that RhlR and CbrA control different properties, lateral spreading and vertical rise, respectively, of a growing biofilm.

The Δ*rhlR*Δ*cbrA* double mutant formed unstable biofilms that readily gave rise to suppressor flares that allowed spreading of the biofilm similar to the Δ*rhlR* mutant (Fig. 2A). We isolated 12 spontaneously arising rugose mutants from Δ*rhlR*Δ*cbrA* colony biofilms and analyzed them by whole genome sequencing. Ten suppressors contained deletions, insertions or missense mutations in the *crc* gene, while the remaining two suppressors harbored mutations in the *rplP* and *rplC* genes respectively (Fig 2A, Table S1). Crc, the carbon catabolite repression protein, is an RNA-binding protein that prevents translation of catabolic enzymes for nonpreferred carbon sources when succinate is present (Pei et al. 2019). Crc is antagonized by small RNA CrcZ whose expression is activated by the CbrA/CbrB two-component system (Fig. 1A) (Sonnleitner et al. 2009). We generated Δ*crc* single, Δ*rhlR*Δ*crc* and Δ*cbrA*Δ*crc* double, and Δ*rhlR*Δ*cbrA*Δ*crc* mutants and analyzed their twitching motility and biofilm forming behaviors. Absence of Crc showed little effect in WT and Δ*rhlR* backgrounds but substantially altered the biofilms of the Δ*cbrA* and

Δ*rhlR*Δ*cbrA* mutants (Fig. 2B). Specifically, deletion of *crc* abolished the vertical rise of the colony biofilm and decreased pellicle formation in the Δ*cbrA* mutant background (Fig. 2B-D, S2A). On the contrary, deletion of *crc* promoted surface area coverage of colony biofilms and increased pellicle production in the Δ*rhlR*Δ*cbrA* double mutant (Fig. 2B-D). Introduction of a plasmid expressing *crc* under its native promoter to the Δ*rhlR*Δ*cbrA*Δ*crc* triple mutant resulted in colony biofilm phenotype identical to the Δ*rhlR*Δ*cbrA* double mutant validating our deletion analysis (Fig. S2B). We conclude that Crc promotes biofilm height when CbrA is inactive and restricts biofilm spreading when both RhlR and CbrA are inactive. Taken together, our data suggest that in the absence of quorum sensing via RhlR and nutrient-sensing signaling via CbrA, Crc functions as a master regulator of biofilm development.

Crc has been reported to promote twitching motility but the molecular mechanism underlying this regulation is unknown (O'Toole et al. 2000). *P. aeruginosa* possesses the type IV pilus (T4P) system for twitching across solid and semisolid surfaces, where the cell extends and retracts multiple pili to pull itself toward the point of attachment (Merz et al. 2000). The pilus is made of repeating subunits of the major pilin protein, PilA (Paranchych et al. 1979). To determine if any of our mutants were defective in twitching motility, we constructed a Δ*pilA* mutant that was impaired in twitching motility compared to WT PA14 (Fig. S3). However, the Δ*rhlR,* Δ*cbrA,* Δ*crc*, Δ*rhlR*Δ*cbrA* double, and Δ*rhlR*Δ*cbrA*Δ*crc* triple mutants were all proficient in twitching motility (Fig. S3). We conclude that under the conditions of our experiments Crc does not control twitching motility. We reason that this difference in phenotype of the Δ*crc* mutant arises due to different media conditions used in the two studies.

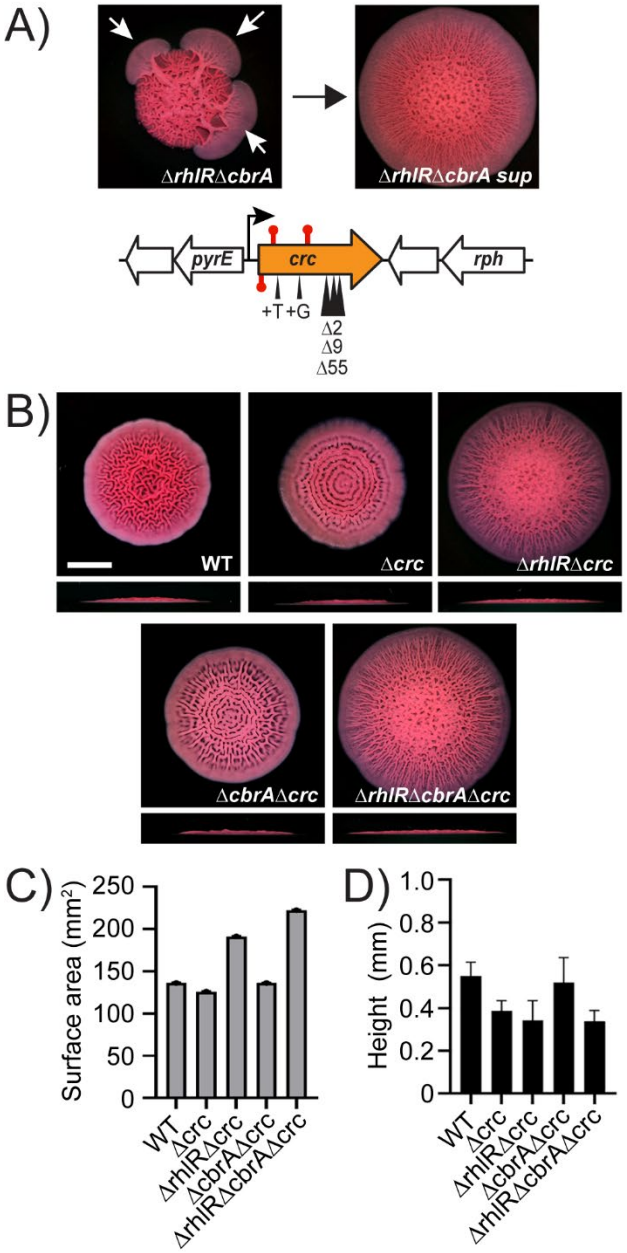

Fig. 2: *P. aeruginosa* Δ*rhlR*Δ*cbrA* double mutant forms unstable biofilms. A) (Top) Shown is a representative isolation of a suppressor mutation of the Δ*rhlR*Δ*cbrA* biofilm phenotype. The white arrows in the left panel indicate flares radiating from the biofilm diagnostic of the emergence of suppressor mutations. The right panel shows the biofilm phenotype of a mutant following isolation. (Bottom) Chromosomal arrangement of the *crc* (orange) gene. Large white arrows represent open reading frames (lengths not to scale), black bent arrow indicates promoter, red stem-loops indicate STOP mutations and black triangles indicate the locations of insertion and deletion suppressor mutations. B) Colony biofilm phenotypes of WT PA14 and the designated mutants on Congo red agar medium after 120 h of growth. Scale bar, 5 mm. C) Colony biofilm surface area quantitation for the indicated strains after 120 h of growth. Error bars represent SEM of three independent experiments. D) Colony biofilm height quantitation for the indicated strains after 120 h of growth. Error bars represent SEM of three independent experiments.

To define the molecular basis underpinning Crc-mediated biofilm regulation and the different Δ*rhlR* and Δ*cbrA* biofilm phenotypes, we used RNA-seq to compare the genomic transcriptional profiles of the biofilms of the WT, Δ*rhlR,* Δ*cbrA,* Δ*crc*, Δ*rhlR*Δ*cbrA* double, and Δ*rhlR*Δ*cbrA*Δ*crc* triple mutants. Total RNAs were extracted from colony biofilms of these mutants after approximately 40 hours of growth on Congo red agar medium. We chose this time point early in the course of biofilm development to avoid spontaneous suppressor mutations in the Δ*rhlR*Δ*cbrA* double mutant. Our comparative transcriptomic analysis revealed that a total 710 genes were differentially expressed by >2-fold (Padj < 0.05 by Benjamini-Hochberg procedure; see Table S2 in the supplemental material) in the Δ*rhlR* mutant (Fig. 3A). Among these genes, 326 overlapped with the CbrA regulon. The CbrA regulon consists of 1367 genes, ~47% of which do not show any overlap with the other mutants tested (Fig. 3A). The Crc regulon consists of 681 genes, of which ~48% are also regulated by CbrA and ~36% coregulated by RhlR (Fig. 3A). Surprisingly, 125 and 174 genes were uniquely regulated in the Δ*rhlR*Δ*cbrA* double and Δ*rhlR*Δ*cbrA*Δ*crc* triple mutants, respectively, suggesting that the combined absence of each regulator gives rise to a cellular response distinct from mere addition of individual regulons. Of the 35 genes that are differentially expressed in every mutant tested here, *phzS* gene and *phzA1-G1* operon encode for enzymes required for phenazine production. Phenazines are redox active secondary metabolites that influence colony biofilm morphology and absence of phenazines confer a hyper-rugose large biofilm phenotype (Fig. S2, Dietrich *et al*, 2013). To determine the contribution of phenazines, we deleted the two phenazine biosynthesis operons (Δ*phz1* and Δ*phz2*; we call this double mutant Δ*phz*) in the WT and the Δ*rhlR*Δ*cbrA* double mutant backgrounds and assayed biofilm formation. In contrast to the Δ*phz* mutant biofilm that spread radially outwards, the Δ*rhlR*Δ*cbrA*Δ*phz* mutant covered less surface area and appeared identical to the Δ*rhlR*Δ*cbrA* double mutant. We conclude that phenazines do not play a role in the biofilm morphology of the Δ*rhlR*Δ*cbrA* double mutant.

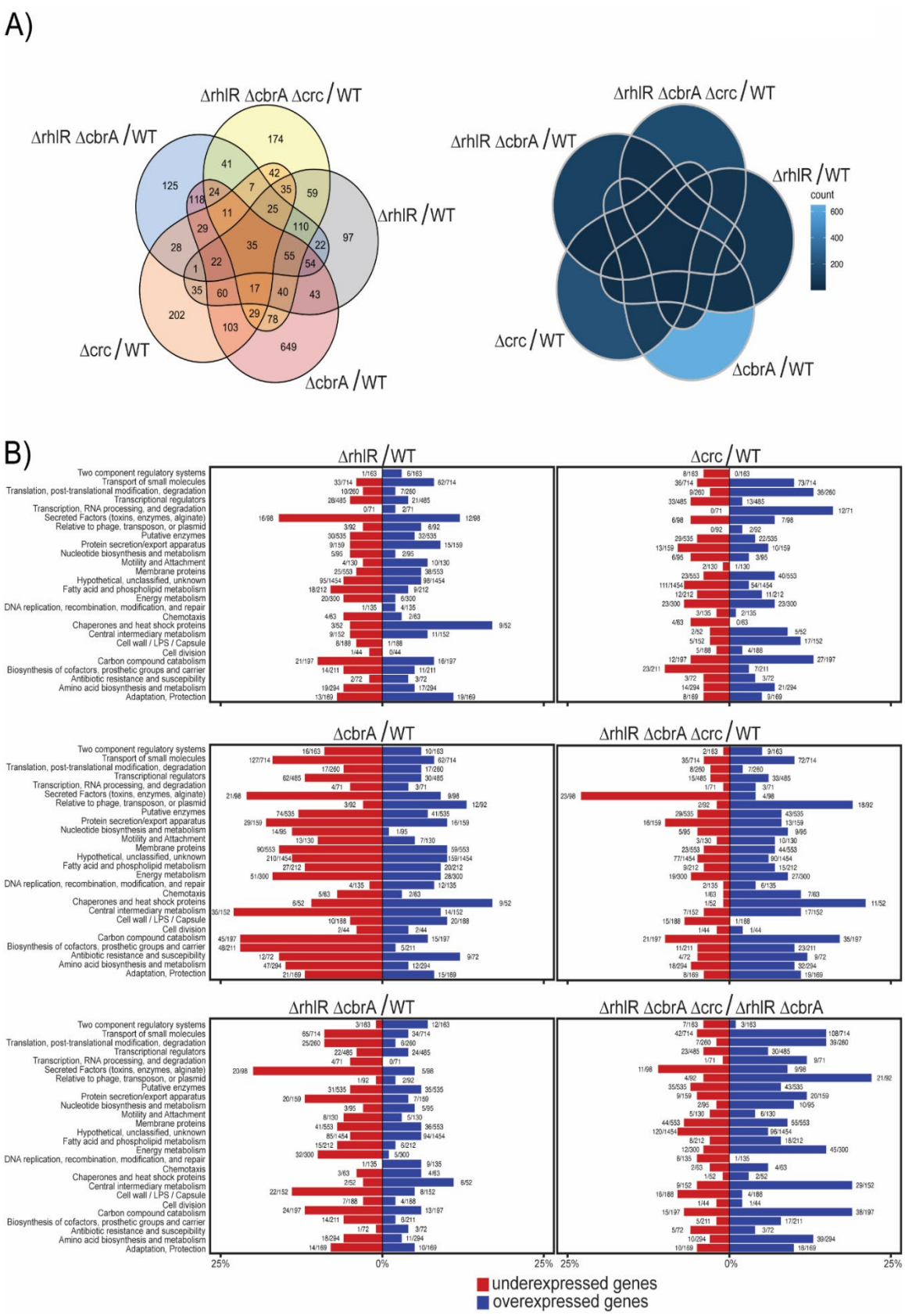

Fig. 3: *P. aeruginosa* Δ*rhlR*Δ*cbrA* double mutant exhibits a transcriptomic profile distinct from its parent Δ*rhlR* and Δ*cbrA* single mutants. A) Venn diagrams showing overlaps in genes that are differentially regulated in Δ*rhlR,* Δ*cbrA,* Δ*crc*, Δ*rhlR*Δ*cbrA* double, and Δ*rhlR*Δ*cbrA*Δ*crc* triple mutants compared to WT. Numbers (left) or shade of blue (right) indicate number genes differentially regulated in each intersection. B) PseudoCAP analysis. Percentage of genes in each PseudoCAP category that are downregulated (red) or upregulated (blue) in Δ*rhlR,* Δ*cbrA,* Δ*crc*, Δ*rhlR*Δ*cbrA* or Δ*rhlR*Δ*cbrA*Δ*crc* compared to WT and Δ*rhlR*Δ*cbrA*Δ*crc* compared to Δ*rhlR*Δ*cbrA*. Numbers next to bars indicated the number of genes up- or downregulated and total number of genes in each PseudoCAP category.

Next, we binned the differentially expressed genes according to their functional categories using PseudoCAP analysis. Shown in Fig. 3B is our analysis; as reported previously, CbrA upregulates the "Carbon compound metabolism", "Amino acid biosynthesis and metabolism", "Central intermediary metabolism" and "Energy metabolism" functional classes. We note that the "Secreted Factors (toxins, enzymes, alginate)" functional class is downregulated in Δ*rhlR,* Δ*cbrA,* Δ*rhlR*Δ*cbrA* and Δ*rhlR*Δ*cbrA*Δ*crc* mutants, highlighting the importance of RhlR and CbrA in *P. aeruginosa* virulence. In addition, CbrA appears to upregulate the "Biosynthesis of cofactors, prosthetic groups, and carriers" class and control the expression of several genes in the "Two component regulatory system", "Transport of small molecules", "Membrane proteins" functional classes. Comparing the Δ*rhlR*Δ*cbrA* and Δ*rhlR*Δ*cbrA*Δ*crc* mutants shows that Crc represses several genes in the "Transport of small molecules", "Energy metabolism", and "Relative to phage, transposon or plasmid" classes only in the Δ*rhlR*Δ*cbrA* double mutant background. However, most of genes regulated by RhlR, CbrA and Crc belong to the "Hypothetical, unclassified, unknown" category limiting the power of our analysis. Nonetheless, overall, the profile of the Δ*rhlR*Δ*cbrA* is similar to the Δ*rhlR* mutant suggesting that absence of RhlR is epistatic to the absence of CbrA for most functional categories.

What biofilm related genes are differentially expressed in all three regulons - RhlR, CbrA and Crc? Production of the extracellular matrix is a defining feature of biofilms, and the matrix composition can vary depending on the bacterial species. *P. aeruginosa* biofilm matrix have been reported to be composed of three different exopolysaccharides – Pel, Psl and alginate –

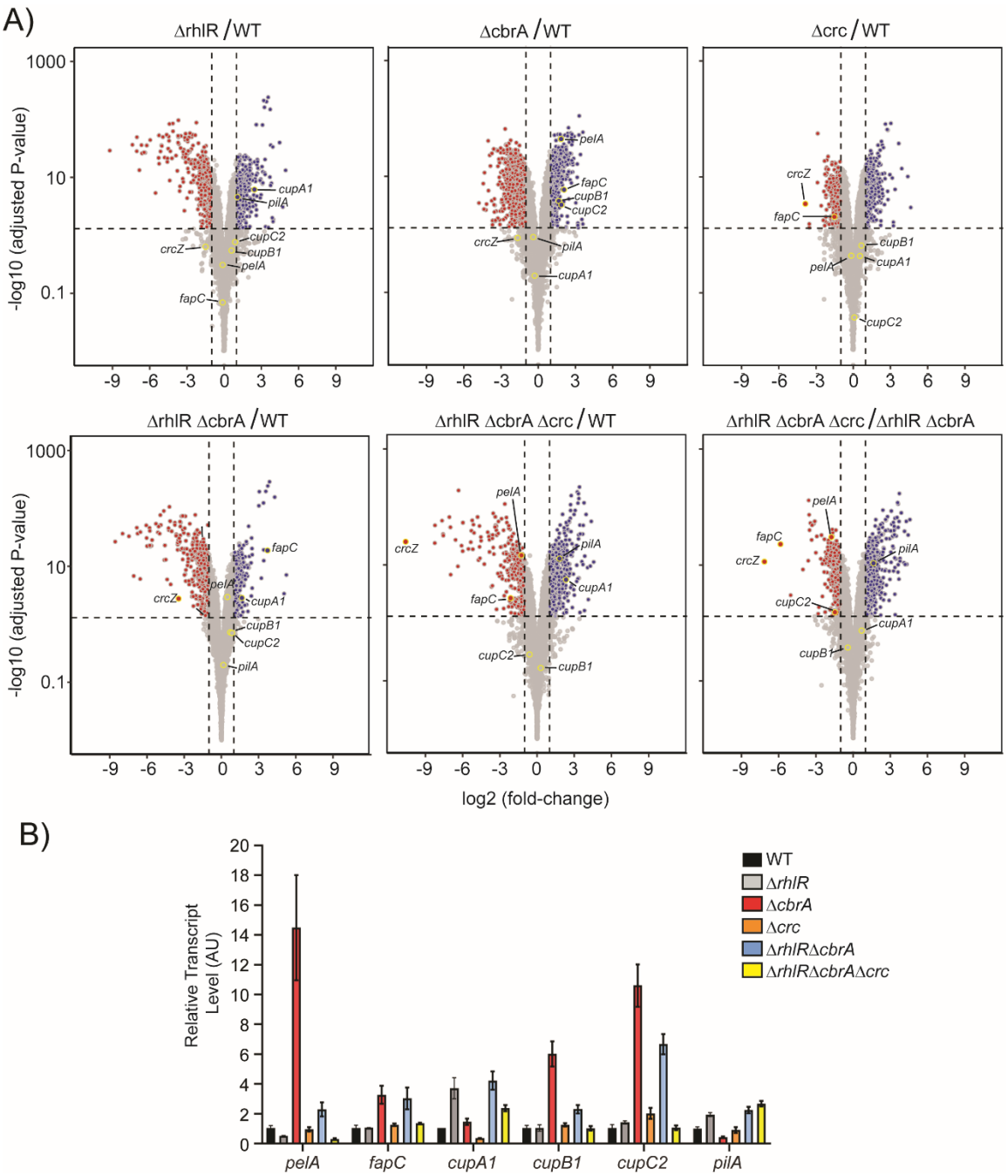

Fig. 4: Matrix components are upregulated in the Δ*cbrA* and Δ*rhlR*Δ*cbrA* mutant biofilms. A) Volcano plots of RNA-seq data for Δ*rhlR,* Δ*cbrA,* Δ*crc*, Δ*rhlR*Δ*cbrA* and Δ*rhlR*Δ*cbrA*Δ*crc* compared to WT, and Δ*rhlR*Δ*cbrA*Δ*crc* compared to Δ*rhlR*Δ*cbrA*. Red circles with gray outlines represent genes with gene expression fold-changes ≤−2 and the P values (Padj), adjusted using the Benjamini-Hochberg procedure, <0.05. Blue circles with gray outlines represent genes with gene expression fold-changes ≥2 and the P values (Padj), adjusted using the Benjamini-Hochberg procedure, <0.05. Gray circles with gray outlines represent genes with gene expression fold changes ≥-2 or ≤2 or Padj ≥ 0.05. Genes of interest are outlined in yellow and labeled. B) Relative expression of the representative biofilm matrix genes *pelA*, *fapC*, *cupA1*, *cupB1*, *cupC2* and *pilA* in colony biofilms of the WT (black), Δ*rhlR* (gray), Δ*cbrA* (red), Δ*crc* (orange), Δ*rhlR*Δ*cbrA*

(blue) and Δ*rhlR*Δ*cbrA*Δ*crc* (yellow) mutants. Data are normalized to *16S RNA, clpX*, *ostA* and *rpsO* as reference in qRT-PCR. Error bars represent SD of three biological replicates. AU denotes arbitrary units.

depending on the strain. In PA14, Pel is the major exopolysaccharide as Psl is not made by this strain and alginate is not a significant component of the biofilm matrix under commonly used laboratory growth conditions (Jennings et al. 2015). In addition, the matrix involves a large arsenal of cell surface-associated structures, including flagella, type IVa or type IVb pili, Fap fibrils and the cup fimbriae (Ruer et al. 2007; de Bentzmann et al. 2006; Klausen et al. 2003; O'Toole and Kolter, 1998; Vallet et al. 2001; Dueholm et al. 2010). *P. aeruginosa* can produce three types of cup fimbriae – CupA, CupB and CupC, products of *cupA*, *cupB*, and *cupC* gene clusters each of which encodes an usher, a chaperone, and at least one fimbrial subunit. Close inspection of the RNA-seq data revealed that Pel, Fap, CupB and CupC matrix components are upregulated in the Δ*cbrA* mutant, while type IVa pili and CupA are upregulated in the Δ*rhlR* mutant (Fig. 4A).

Differential expression of selected biofilm-associated genes by RhlR, CbrA or Crc in the RNAseq experiment was validated by quantitative Real Time PCR analysis. A comparison between Fig. 3A and 3B shows that the results obtained match the RNAseq data, since the mRNA levels of the *pelA*, *fapC*, *cupB1* and *cupC2* genes increased in the Δ*cbrA* single and Δ*rhlR*Δ*cbrA* double mutants but decreased in the Δ*rhlR*Δ*cbrA*Δ*crc* triple mutants. This suggests that Crc promotes the production of Pel, Fap, CupB and CupC matrix components but only in the absence of CbrA. Taken together, our data suggests a model where Crc can function as an activator of biofilm matrix components when it is not antagonized by CrcZ sRNA (Sonnleitner et al. 2009).

Carbon catabolite repression is widespread in bacteria. However, the CbrA/CbrB and Crc proteins are thought to be present only in Pseudomonads. We wondered if any bacteria outside of the Pseudomonaceae family also encoded for any of these proteins involved in nutritional adaptation. As a first step, we used blastp analysis using PA14 CbrA amino acid sequence and mapped CbrA orthologs on the microbial tree of life derived by GTDB (Fig. 5). The majority of

these CbrA orthologs are present in two bacterial phyla – Proteobacteria and Bacteroidota, suggesting that CbrA is more widely distributed than previously reported. We next asked which of these CbrA containing bacteria also encode for Crc. We note that the majority of these bacteria possesses both CbrA and Crc. We therefore propose that the signaling pathway of CbrA -> CbrB -> Crc is used by diverse bacteria to sense and respond to nutritional cues.

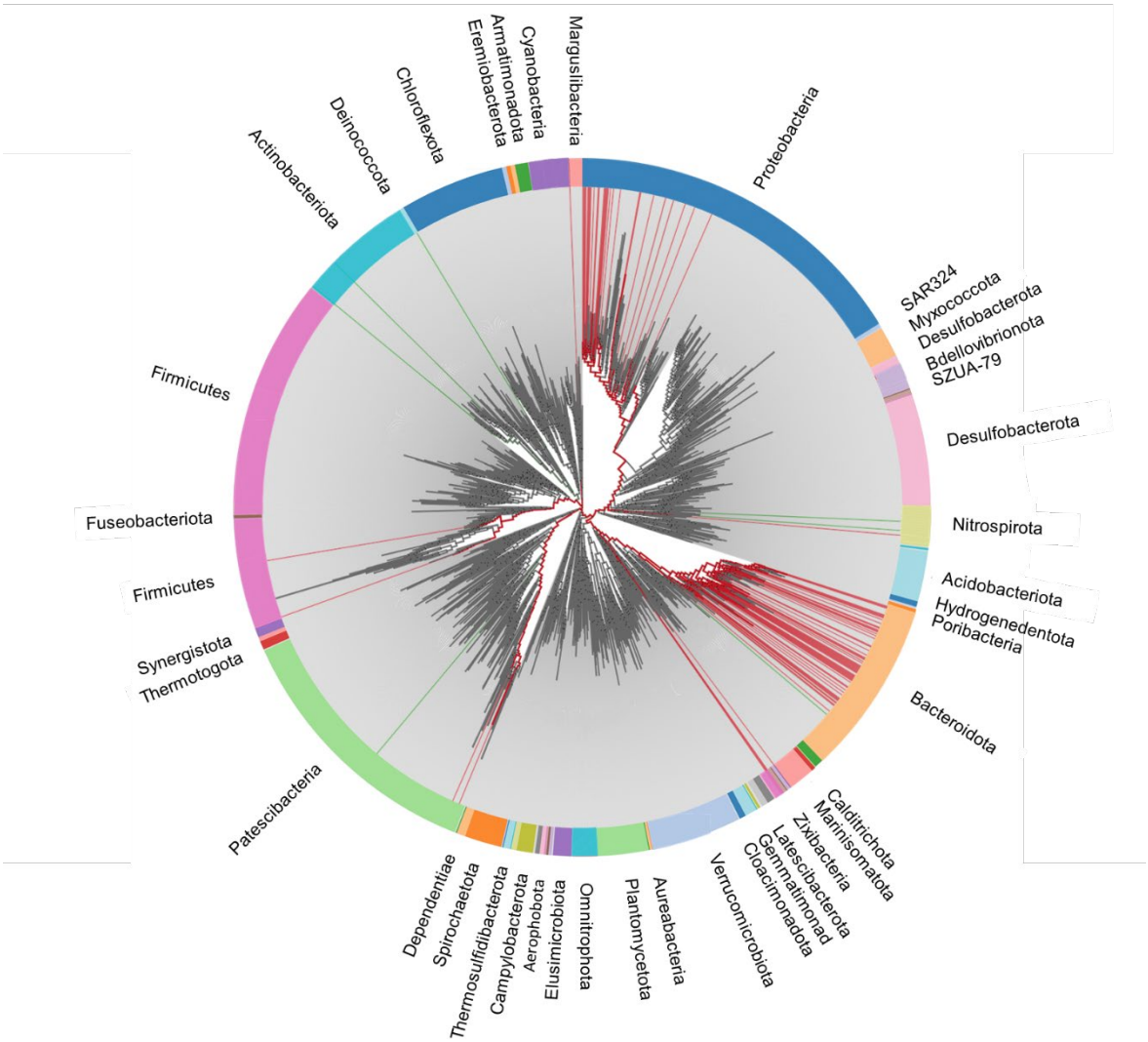

Fig. 5: CbrA and Crc proteins are widely conserved in Proteobacteria and Bacteroidota phyla. Each branch of the tree represents a specific family. If a species contained a homolog for both *cbrA* and *crc*, the family of that species is highlighted in red. Lineages with at least one species that contained a homolog for *cbrA* but not *crc* are highlighted in green.

MATERIALS AND METHODS

Strains and growth conditions. *P. aeruginosa* UCBPP-PA14 strain was grown in lysogeny broth (LB) (10 g tryptone, 5 g yeast extract, 5 g NaCl per L), in 1% Tryptone broth (TB) (10 g tryptone per L) and on LB plates fortified with 1.5% Bacto agar at 37˚C. When appropriate, antimicrobials were included at the following concentrations: 400 µg/mL carbenicillin, 50 µg/mL gentamycin, 100 µg/mL irgasan.

Strain construction. Strains and plasmids were constructed as described previously (Mukherjee et al. 2017). To construct marker-less in-frame chromosomal deletions in *P. aeruginosa*, DNA fragments flanking the gene of interest were amplified, assembled by the Gibson method, and cloned into pEXG2 (Hmelo et al., 2015). The resulting plasmids were used to transform *Escherichia coli* SM10λ*pir*, and subsequently, mobilized into *P. aeruginosa* PA14 via biparental mating. Exconjugants were selected on LB containing gentamicin and irgasan, followed by recovery of deletion mutants on LB medium containing 5% sucrose. Candidate mutants were confirmed by PCR. The *cbrA* complementation plasmid was constructed by inserting DNA containing the promoter of *dksA* and the entire *cbrA* open-reading frame using HindIII and XbaI, followed by cloning into similarly digested pUCP18.

Colony biofilm assay. One microliter of overnight *P. aeruginosa* cultures grown at 37°C in 1% Tryptone broth was spotted onto 60 x 15 mm Petri plates containing 10 mL 1% Tryptone medium fortified with 40 mg per L Congo red and 20 mg per L Coomassie brilliant blue dyes, and solidified with 1% agar. Colonies were grown at 25°C and images were acquired after 120 h using a Zeiss AxioZoom v16 microscope.

Pellicle biofilm assay. *P. aeruginosa* was cultured overnight in 200 ul LB in a BioTek Synergy Neo2 microplate reader at 37°C under shaking conditions. The OD600 of the culture was taken by the plate reader to calculate the amount of culture needed to inoculate 2 ml 1% Tryptone broth so that the final OD is 0.005. Pellicle biofilms were developed for 96 hours in stationary 16*100 mm glass test tubes at room temperature.

RNA-seq. *P. aeruginosa* colony biofilms were grown for 40 h before harvested with a plastic inoculation loop. Half of each biofilm was picked up and transferred into 600 ul of Tri-reagent (Zymo Research) and disrupted by pipetting with a 1 ml tip. Total RNA was extracted with the Zymo Direct-zol RNA kit following the manufacturer's instructions. Samples were subjected to DNAse treatment using Ambion DNase I (RNase-free) kit, followed by rRNA depletion and library preparation with Illumina Stranded Total RNA Prep with Ribo-Zero kit. Libraries were sequenced on Illumina's NextSeq 2000, with 51 bp paired-end reads and 10 bp long index reads (51-10-10-51).

RNA-seq analysis. RNA-seq reads were processed using the nf-core RNAseq pipeline version 3.4. Briefly, low-quality bases and contaminant adapters were trimmed using Cutadapt version 3.4 and Trimgalore version 0.6.7. RNA-seq reads passing quality filters were mapped against the reference genome of *P. aeruginosa* UCBPP_PA14 strain (GenBank assembly accession number CP000438.1) using HISAT2 version 2.2.0 (with parameters --rna-strandness RF, --no-mixed, --no-discordant, --no-spliced-alignment; Kim et al., 2019). Next, read mappings for each annotated gene were counted using the featureCounts program within the Subread package version 2.0.1 (with parameters -B -C and -s 2, Liao et al. 2014). Analysis of differentially expressed genes was performed using the DESeq2 package 1.28.0 (Love et al. 2014). Genes were considered significantly differentially expressed when the gene expression fold change was ≥2 or was ≤−2 and the P value (Padj), adjusted using the Benjamini-Hochberg procedure, was <0.05. Venn

diagrams in Figure 3 were generated using the venn and ggVennDiagram (Gao et al. 2021) packages.

qRT-PCR. *P. aeruginosa* colony biofilms were grown for 40 h before harvested with a plastic inoculation loop. Half of each biofilm was picked up and transferred into 600 ul of Tri-reagent (Zymo Research) and disrupted by pipetting with a 1 ml tip. Total RNA was extracted with the Zymo Direct-zol RNA kit following the manufacturer's instructions and quantified with a BioTek Synergy Neo2 microplate reader. 0.5 µg of total RNA was used for reverse-transcription using the TaKaRa PrimeScript RT Reagent Kit with gDNA Eraser. The resulting cDNA was used for real-time PCR using the Applied biosystems PowerTrack SYBR Green Master Mix on a Bio-Rad C1000 Touch Thermal Cycler. The results were exported into RDML v1.1 format and analyzed with web-based LinRegPCR (https://www.gear-genomics.com/rdml-tools/). Relative fold change was calculated with the qBase method (Hellemans et al. 2007) using *16s, clpX*, *ostA* and *rpsO* as reference genes.

Phylogenetic analysis. To generate the phylogenetic tree, we first ran a blastp using the PA14 amino acid sequence of CbrA. Using only hits with values over 30% identity and 60% sequence coverage, we generated a list of several hundred cbrA homologs across many species. This list was then filtered to not include duplicates and nonspecific hits (ex. Gamma-proteobacterium). The species with CbrA homologs were then used to create a local blast database. Using this local database, we ran another blastp for the PA14 sequence of Crc. We again only counted the protein as a homolog if it met the standard of 30% identity and 60% sequence coverage (Table S5). Using this data and annotree, we annotated the microbial tree of life derived by GTDB to show which families contained species with a hit for either only *cbrA* or both *cbrA* and *crc*.

ACKNOWLEDGEMENTS We thank Eric Littman and the Genomics Core Facility at the University of Chicago for help with whole genome sequencing analyses.

REFERENCES

Brint JM, Ohman DE. 1995. Synthesis of multiple exoproducts in *Pseudomonas aeruginosa* is under the control of RhlR-RhlI, another set of regulators in strain PAO1 with homology to the autoinducer-responsive LuxR-LuxI family. *J. Bacteriol.* 177: 7155–7163.

Capra EJ, Laub MT. 2012.Evolution of two-component signal transduction systems. *Annu Rev Microbiol*. 66:325-47.

Davies DG, et al. 1998. The involvement of cell-to-cell signals in the development of a bacterial biofilm. *Science* 280:295-8.

de Bentzmann S, Aurouze M, Ball G, Filloux A. FppA, a novel *Pseudomonas aeruginosa* prepilin peptidase involved in assembly of type IVb pili. *J Bacteriol*. 2006 Jul;188(13):4851-60.

Dietrich LEP, Okegbe C, Price-Whelan A, Sakhtah H, Hunter RC, Newmana DK (2013) Bacterial community morphogenesis is intimately linked to the intracellular redox state. *J Bacteriol* 195: 1371–1380

Dueholm MS, Petersen SV, Sønderkær M, Larsen P, Christiansen G, Hein KL, Enghild JJ, Nielsen JL, Nielsen KL, Nielsen PH, Otzen DE. Functional amyloid in *Pseudomonas*. *Mol Microbiol*. 2010 Aug;77(4):1009-20.

Flemming, HC, et al. 2016. Biofilms: An emergent form of bacterial life. *Nat. Rev. Microbiol.* 14, 563–575.

Gao CH, Yu G, Cai P. ggVennDiagram: An Intuitive, Easy-to-Use, and Highly Customizable R Package to Generate Venn Diagram. *Front Genet*. 2021 Sep 7;12:706907.

Hall-Stoodley L, et al. 2004. Bacterial biofilms: from the natural environment to infectious diseases. *Nat. Rev. Microbiol.* 2: 95

Hellemans J, Mortier G, De Paepe A, Speleman F, Vandesompele J. qBase relative quantification framework and software for management and automated analysis of real-time quantitative PCR data. Genome Biol. 2007;8(2):R19.

Hmelo, L.R., Borlee, B.R., Almblad, H., Love, M.E., Randall, T.E., Tseng, B.S., Lin, C., Irie, Y., Storek, K.M., Yang, J.J., et al. (2015). Precision-engineering the *Pseudomonas aeruginosa* genome with two-step allelic exchange. Nat. Protoc. *10*, 1820–1841.

Jennings LK, Storek KM, Ledvina HE, Coulon C, Marmont LS, Sadovskaya I, Secor PR, Tseng BS, Scian M, Filloux A, Wozniak DJ, Howell PL, Parsek MR. Pel is a cationic exopolysaccharide that cross-links extracellular DNA in the *Pseudomonas aeruginosa* biofilm matrix. *Proc Natl Acad Sci U S A*. 2015 Sep 8;112(36):11353-8.

Karygianni L, et al. 2020. Biofilm Matrixome: Extracellular Components in Structured Microbial Communities. *Trends Microbiol.* 28, 668-681.

Kim D, Paggi JM, Park C, Bennett C, Salzberg SL. Graph-based genome alignment and genotyping with HISAT2 and HISAT-genotype. Nat Biotechnol. 2019 Aug;37(8):907-915.

Kim M, et al. 2015. *Pseudomonas aeruginosa* wound infection involves activation of its iron acquisition system in response to fascial contact. *J Trauma Acute Care Surg.* 78(4):823-829.

Klausen M, Heydorn A, Ragas P, Lambertsen L, Aaes-Jørgensen A, Molin S, Tolker-Nielsen T. Biofilm formation by *Pseudomonas aeruginosa* wild type, flagella and type IV pili mutants. *Mol Microbiol.* 2003 Jun;48(6):1511-24.

Liao Y, Smyth GK, Shi W. featureCounts: an efficient general purpose program for assigning sequence reads to genomic features. *Bioinformatics*. 2014 Apr 1;30(7):923-30.

Liu C, Sun D, Zhu J, Liu W. Two-Component Signal Transduction Systems: A Major Strategy for Connecting Input Stimuli to Biofilm Formation. *Front Microbiol*. 2019 Jan 10;9:3279.

Love MI, Huber W, Anders S. Moderated estimation of fold change and dispersion for RNA-seq data with DESeq2. *Genome Biol*. 2014;15(12):550.

Manfredi R, et al. 2000. Pseudomonas spp. Complications in patients with HIV disease: an eight-year clinical and microbiological survey. *Eur. J. Epidemiol*. 16:111-8.

Markou P, Apidianakis Y. 2014. Pathogenesis of intestinal *Pseudomonas aeruginosa* infection in patients with cancer. *Front. Cell. Infect. Microbiol.* 3:115.

Mendler K, et al. 2019. AnnoTree: visualization and exploration of a functionally annotated microbial tree of life. *Nucleic Acids Research* 47:4442-4448.

Merz AJ, So M, Sheetz MP. Pilus retraction powers bacterial twitching motility. *Nature*. 2000 Sep 7;407(6800):98-102.

Miller MB, Bassler BL (2001) Quorum Sensing In Bacteria. *Annu Rev Microbiol* 55: 165–199

Monteagudo-Cascales E, et al. 2022. The Regulatory Hierarchy Following Signal Integration by the CbrAB Two-Component System: Diversity of Responses and Functions. *Genes* (Basel) 13(2):375.

Mukherjee, S., Moustafa, D., Smith, C.D., Goldberg, J.B., and Bassler, B.L. (2017). The RhlR quorum-sensing receptor controls *Pseudomonas aeruginosa* pathogenesis and biofilm development independently of its canonical homoserine lactone autoinducer. *PLoS Pathog*. *13*, 1–25.

Mukherjee S, et al. 2018. PqsE and RhlR are an autoinducer synthase-receptor pair that control virulence and biofilm development in *Pseudomonas aeruginosa*. *Proc. Natl. Acad. Sci. USA* 115(40): E9411-E9418.

Mukherjee, S., and Bassler, B.L. (2019). Bacterial quorum sensing in complex and dynamically changing environments. *Nat. Rev. Microbiol*. *17*, 371–382.

O'Toole GA, Gibbs KA, Hager PW, Phibbs PV Jr, Kolter R. The global carbon metabolism regulator Crc is a component of a signal transduction pathway required for biofilm development by *Pseudomonas aeruginosa. J Bacteriol*. 2000 Jan;182(2):425-31.

O'Toole GA, Kolter R. Flagellar and twitching motility are necessary for *Pseudomonas aeruginosa* biofilm development. *Mol Microbiol*. 1998 Oct;30(2):295-304.

Paranchych W, Sastry PA, Frost LS, Carpenter M, Armstrong GD, Watts TH. Biochemical studies on pili isolated from *Pseudomonas aeruginosa* strain PAO. *Can J Microbiol*. 1979 Oct;25(10):1175-81.

Pearson JP, et al. 1995. A second N-acylhomoserine lactone signal produced by *Pseudomonas aeruginosa*. *Proc. Natl. Acad. Sci. USA*. 92: 1490–1494.

Pei XY, et al. 2019. Architectural principles for Hfq/Crc-mediated regulation of gene expression. *Elife* 8:e43158.

Pendleton JN, et al. 2013. Clinical relevance of the ESKAPE pathogens. *Expert. Rev. Anti-Infective Therapy*. 1: 297-308.

Prüß, B.M. (2017). Involvement of Two-Component Signaling on Bacterial Motility and Biofilm

Development. *J. Bacteriol*. *199*, 1–12.

Ruer S, Stender S, Filloux A, de Bentzmann S. Assembly of fimbrial structures in *Pseudomonas aeruginosa:* functionality and specificity of chaperone-usher machineries. *J Bacteriol*. 2007 May;189(9):3547-55.

Rumbaugh KP, Griswold JA, Hamood AN (2000) The role of quorum sensing in the in vivo virulence of *Pseudomonas aeruginosa*. *Microbes Infect* 2: 1721–1731

Rutherford, S.T., and Bassler, B.L. (2016). Bacterial Quorum Sensing : Its Role in Virulence and Possibilities for Its Control. 1–26.

Saha CK, et al. 2021. Rodrigo Sanches Pires, Harald Brolin, Maxence Delannoy, Gemma Catherine Atkinson, FlaGs and webFlaGs: discovering novel biology through the analysis of gene neighbourhood conservation. *Bioinformatics*, 37:1312–1314.

Sakuragi Y, Kolter R. 2007. Quorum-sensing regulation of the biofilm matrix genes (pel) of *Pseudomonas aeruginosa*. *J Bacteriol* 189: 5383–5386

Seed PC, et al. 1995. Activation of the *Pseudomonas aeruginosa lasI* gene by LasR and the *Pseudomonas* autoinducer PAI: An autoinduction regulatory hierarchy. *J. Bacteriol.* 177: 654–659.

Sonnleitner E, et al. 2009. Small RNA as global regulator of carbon catabolite repression in *Pseudomonas aeruginosa. Proc Natl Acad Sci USA.* 106(51):21866-71.

Sonnleitner E, et al. 2018. Interplay between the catabolite repression control protein Crc, Hfq and RNA in Hfq-dependent translational regulation in *Pseudomonas aeruginosa*. *Nucleic Acids Res*. 46(3):1470-1485

Vallet I, Olson JW, Lory S, Lazdunski A, Filloux A. The chaperone/usher pathways of *Pseudomonas aeruginosa*: identification of fimbrial gene clusters (cup) and their involvement in biofilm formation. *Proc Natl Acad Sci U S A*. 2001 Jun 5;98(12):6911-6.

Wang BX, et al. 2021. Two-Component Signaling Systems Regulate Diverse Virulence-Associated Traits in *Pseudomonas aeruginosa*. *Appl Environ Microbiol*. 11;87(11):e03089-20.

Yeung AT, et al. 2011. The sensor kinase CbrA is a global regulator that modulates metabolism, virulence, and antibiotic resistance in *Pseudomonas aeruginosa. J Bacteriol.*193(4):918-31.

SUPPLEMENTAL FIGURES

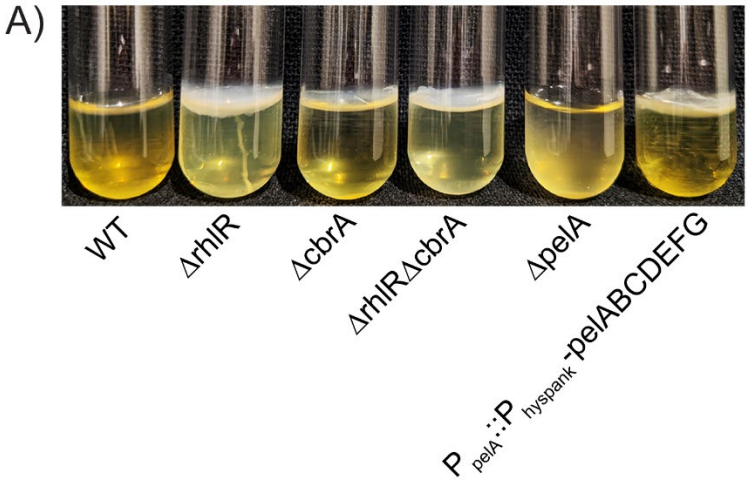

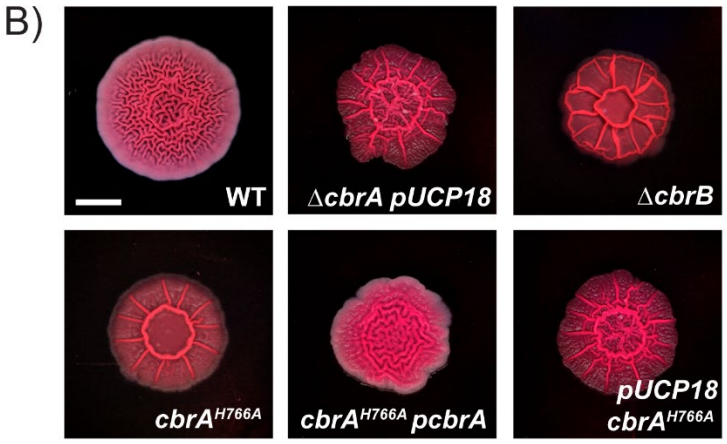

Supplemental Fig. 1: A) Pellicle biofilms of the indicated *P. aeruginosa* mutants imaged after 96 h of growth in standing cultures. B) Colony biofilm phenotypes of the designated mutants on Congo red agar medium after 120 h of growth.

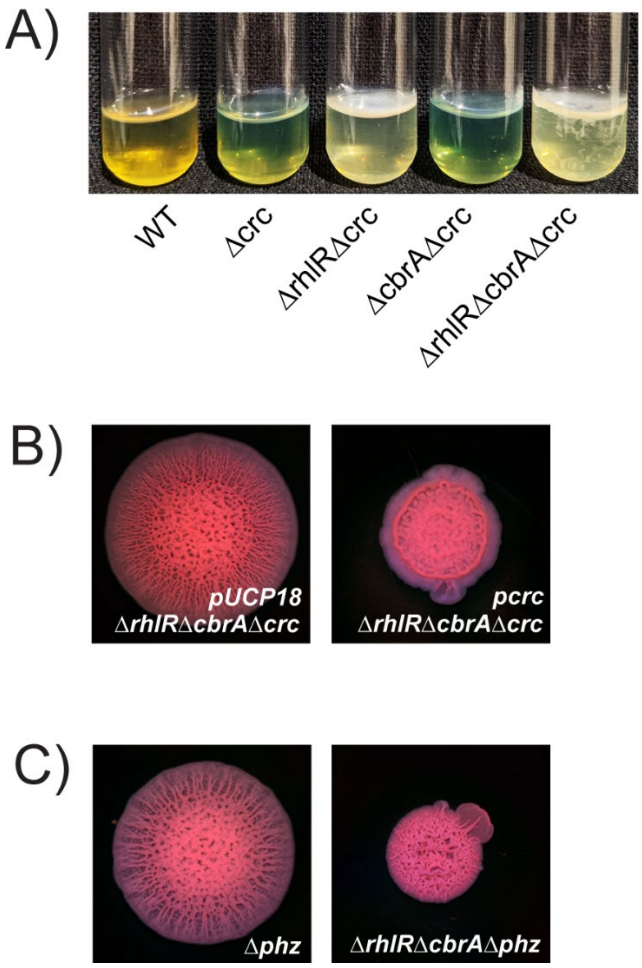

Supplemental Fig. 2: A) Pellicle biofilms of the indicated *P. aeruginosa* mutants imaged after 96 h of growth in standing cultures. B-C) Colony biofilm phenotypes of the designated mutants on Congo red agar medium after 120 h of growth.

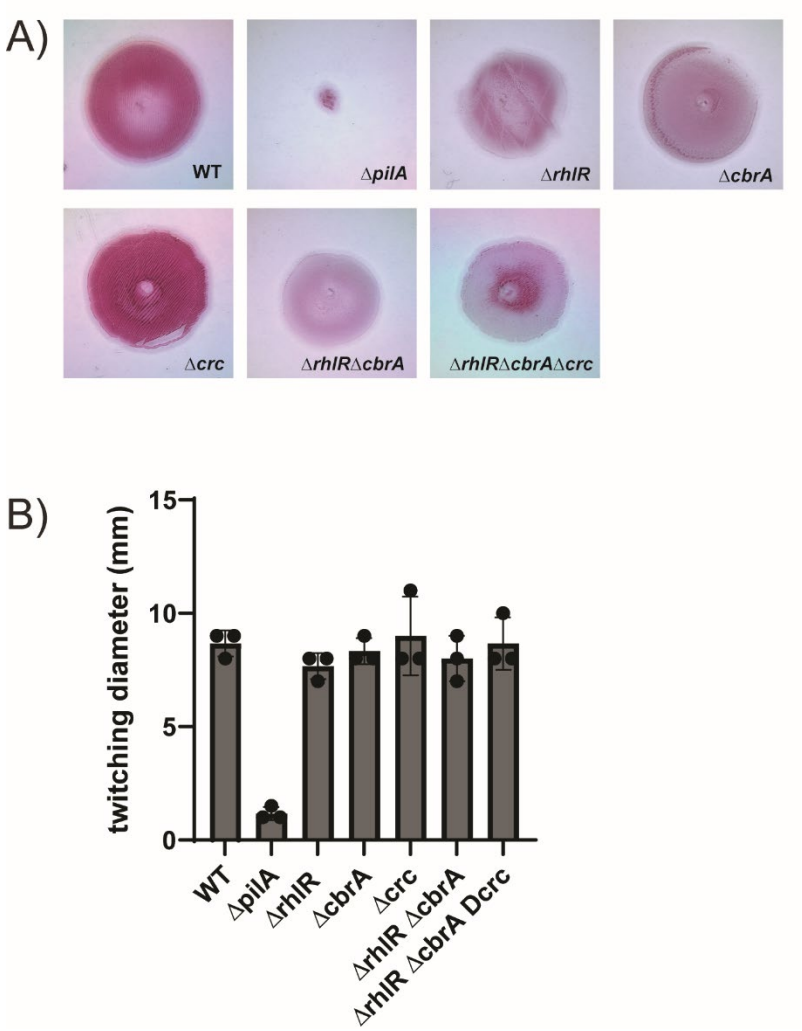

Supplemental Fig. 3: A) Twitching motility zones of the WT PA14 and indicated mutants imaged after crystal violet staining. B) Twitching zone quantification for WT and indicated mutants. Error bars represent SD of three biological replicates.